Proceedings of SPIE, Vol. 4742, April 2002

Characterization of Elastic Wave Propagation in Soil

Gregg D. Larson[a], James S. Martin[a], Waymond R. Scott, Jr.[b],
George S. McCall II[c], and Peter H. Rogers[a]
Georgia Institute of Technology
[a]Woodruff School of Mechanical Engineering
[b]School of Electrical and Computer Engineering
[c]Georgia Tech Research Institute
Atlanta, Georgia 30332

ABSTRACT

To optimize a landmine detection system currently being developed at Georgia Tech that uses both electromagnetic and elastic waves, wave propagation in soils has been studied to evaluate propagation characteristics and to identify nonlinear mechanisms. The system under development generates elastic waves in the soil using a surface-contacting transducer designed to preferentially excite Rayleigh waves, thus interrogating the surface layers of the soil. These waves propagate through the region of interest and interact with buried landmines and typical clutter objects (i.e., rocks, sticks, and man-made objects). Surface displacements are measured using a non-contact radar sensor that is scanned over the region of interest. To characterize the wave propagation effects as a function of drive amplitude and as a function of input signal type, a series of experiments was conducted using the radar sensor, accelerometers, and geophones at two test sites, the experimental model at Georgia Tech and a field test site at the Georgia Tech Research Institute's Cobb County Research Facility in suburban Atlanta. The two test sites presented different soils as the experimental model uses damp, compacted sand as a soil surrogate while the field test site has a well-weathered mixture of sand, silt, and clay. Surface displacement measurements were made using the radar sensor while both surface and subsurface measurements were made using triaxial accelerometers and geophones. Linear and nonlinear dispersion, wave speed changes, and nonlinear saturation were observed in the measured data.

INTRODUCTION

A landmine detection technique[1-4] has been investigated at Georgia Tech that employs both electromagnetic and elastic waves synergistically to detect propagating waves and their interactions with buried landmines and typical buried and surface clutter. The prototype system has been developed and tested extensively in a laboratory experimental model with controlled environmental conditions using damp, compacted sand as a soil surrogate. Currently, efforts are underway to transition the system testing and development from the laboratory experimental model to a variety of field test sites in order to evaluate system performance in typical environments of interest for demining operations.

The prototype system excites elastic waves in the test region and measures the corresponding surface displacements using a non-contact radar sensor that is scanned over the region of interest using a computer-controlled, three-axis positioner, thus creating a synthetic array of radar sensors. The elastic waves are generated using an electrodynamic transducer coupled to the ground by a long, narrow aluminum bar (30 cm long, 3.2 cm wide, 3.2 cm tall) to preferentially excite Rayleigh surface waves so that the near-surface soil layers are interrogated. The elastic waves propagate through the test region and interact with buried objects (i.e., landmines, rocks, sticks, and man-made objects) causing changes in the propagating waves. The interactions of the elastic waves with buried landmines cause scattered waves as well as resonant oscillations of the mine and soil system; both of these effects can be used as detection cues for the prototype system. Anti-personnel (AP) and anti-tank (AT) mines have been successfully detected in the presence of buried clutter and surface cover (i.e., pine straw) in a range of experimental measurements.

During the course of the system development, several propagation effects have been observed experimentally. Linear and nonlinear dispersion, nonlinear saturation, and changes in propagation speed are evident in the data from the laboratory experimental model and in similar soil at a field test site at the Naval Postgraduate School in Monterey, California[5]. To study these effects in a range of soil types, experiments have been conducted using the radar, triaxial accelerometers, and triaxial geophones in damp, compacted sand and in a well-weathered mixture of sand, silt, and clay.

TEST SITES AND MEASUREMENT FACILITIES

The two sites, the laboratory experimental model[1-4] on the campus of Georgia Tech in Atlanta, Georgia, and a field test site at the Georgia Tech Research Institute's Cobb County Research Facility in Smyrna, Georgia, presented different environmental conditions, elastic properties, soil types, and ambient noise sources for this study of elastic wave propagation. A portable measurement system was developed to study the propagation of elastic waves using both non-contacting and buried sensors.

The laboratory experimental model[1, 6] contains 50 tons of damp, compacted sand and is located on the Georgia Tech campus. Sand was chosen as the soil surrogate as it affords maximum flexibility and repeatability for experimental measurements. Objects can be easily buried without excessive disruption of the sand and reconditioning of the model permits direct comparisons to data from different measurements. While the experimental model contains a single soil type, it is not a perfectly homogeneous medium as it has depth-dependent material properties[6] and a water table maintained approximately 50 to 60 cm below the surface. Ambient noise generated by machinery in nearby laboratories and equipment rooms is predominantly comprised of frequencies below 100 Hz.

The field test site, shown in Figure 1, presented very different soil properties and composition in comparison to the experimental model. Measurements were conducted at

the top of the hill shown in the panoramic view of Figure 1a. The overhead photograph of the site in Figure 1b shows the proximity of local buildings to the test site on the "grassy knoll." The soil was a well-weathered mixture of sand, silt, and clay (commonly referred to as Georgia red clay) with topsoil and grass. For the purposes of these tests, the grass and topsoil were removed from the test region. Soil testing[7] of the site indicated that a five-story building could be built on the site in its current state as the ground is very stiff. An adjacent military airbase and a nearby railroad line presented ambient noise sources of particular interest to the project. Rain noise was also measured during the testing.

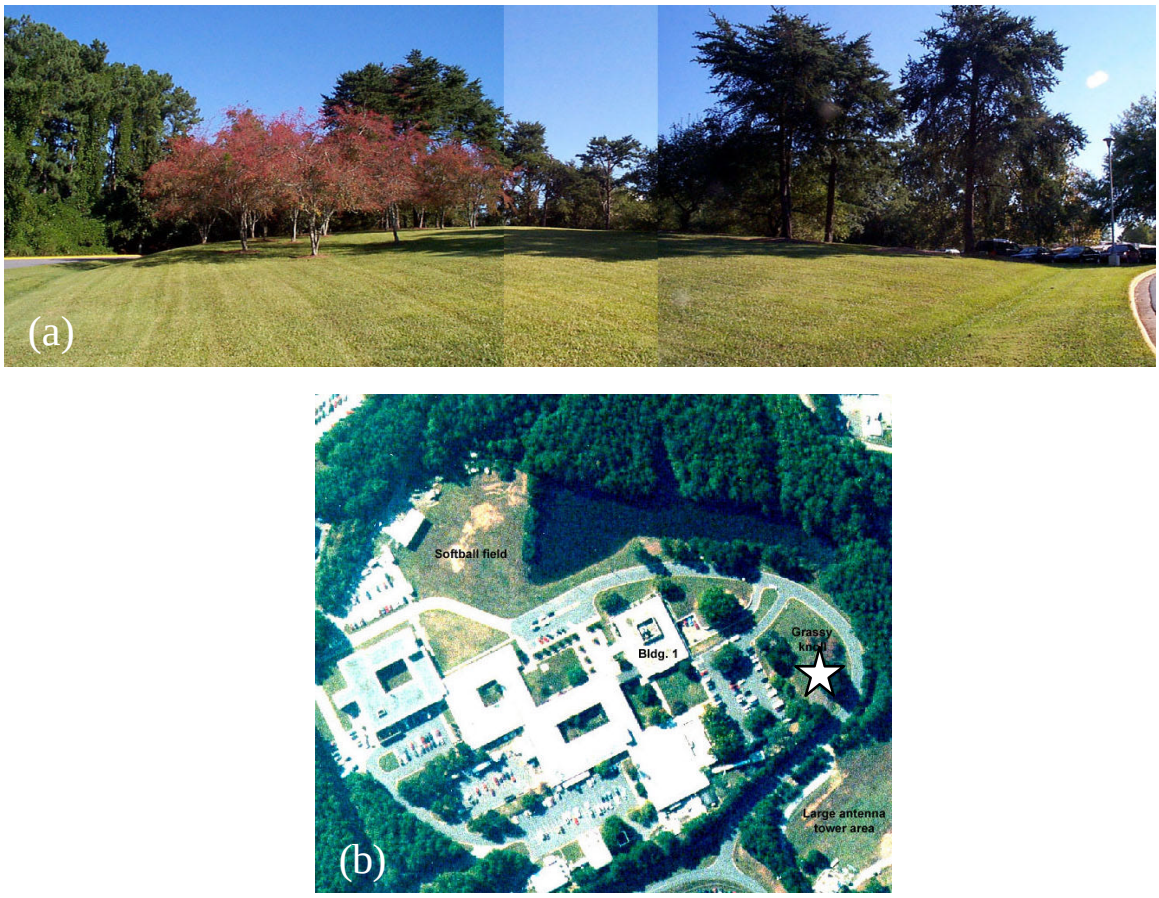

Figure 1: Photographs of Field Test Site at The Georgia Tech Research Institute's Cobb County Research Facility (GTRI-CCRF), (a) Panoramic View and (b) Aerial View. The measurement site is indicated in the aerial view by a star.

A portable measurement system was assembled for field testing which included triaxial accelerometers, triaxial geophones, non-contact radar sensors, a three-axis positioner, electronics, and personal-computer-based data acquisition hardware and software. The triaxial accelerometers, shown in Figure 2a, PCB W356A12 ICP sensors, provided high sensitivity (100 mV/g) in a small package (a cube with 1.27 cm sides) so

that installation of accelerometer arrays would not disturb the existing soil conditions excessively. Initial testing of these accelerometers indicated the need for electrical insulation to decouple significant power line harmonics that were present in the ground at the field site. The triaxial geophones, shown in Figure 2b, 10 Hz resonant Sensor Nederland SM-7 types, were housed in cases for surface mounting and were coupled to the ground by three spikes on the underside of the case. While the geophones as configured in their cases are much larger than the accelerometers, both sensors are much smaller than a wavelength in their intended frequency bands (below 200 Hz for the geophones and between 100 Hz and 1500 Hz for the accelerometers). The radar sensor and three-axis positioner currently used in the experimental model[1] were duplicated in a portable system for field measurements, shown in Figure 2c. LabVIEW software and National Instruments data acquisition and control hardware were used to acquire up to 64 channels simultaneously. Filtering and amplification were accomplished with a Krohn-Hite 3944 Programmable Filter (lowpass filtering), two Stanford Research SR560 preamplifiers (bandpass filtering and amplification), Frequency Devices Programmable Filters (lowpass filtering), and custom-built preamplifiers (amplification for geophones).

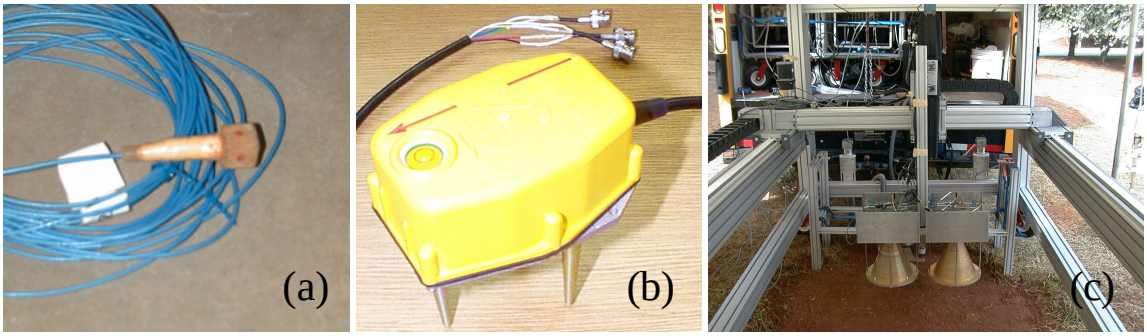

Figure 2: Sensors Used in Measurements, (a) Triaxial Accelerometers, (b) Triaxial Geophones, and (c) Radar Sensor on Three-Axis Positioner.

EXPERIMENTAL MEASUREMENTS

In a series of tests in the experimental model, measurements covering a range of drive signal amplitudes revealed linear and nonlinear dispersion, wave speed changes, and nonlinear saturation. Waterfall plots of the data measured with the radar sensor with low and high drive amplitude drive signals are shown in Figure 3. Each trace plotted in Figure 3 represents the measured surface displacement as a function of time at a location in the experimental model. The trace at the bottom of each figure was measured 37 cm from the elastic wave source while the trace at the top of each figure was measured 180 cm further away. The vertical spacing between traces is 1 cm. For this measurement, a differentiated Gaussian pulse with a center frequency of 450 Hz was averaged 1000 times. Comparison of the measurements made at low and high drive amplitudes indicates substantial differences caused by the drive amplitudes. There are two waves apparent in the data, the leaky surface wave[8] and the Rayleigh wave. While both waves are present in the data shown in Figure 3, there is a substantially more complicated wave field

apparent in the high drive amplitude waterfall. In the experimental model, the leaky surface waves propagate in the range of 180 to 200 m/s and the Rayleigh wave propagates from 80 to 100 m/s.

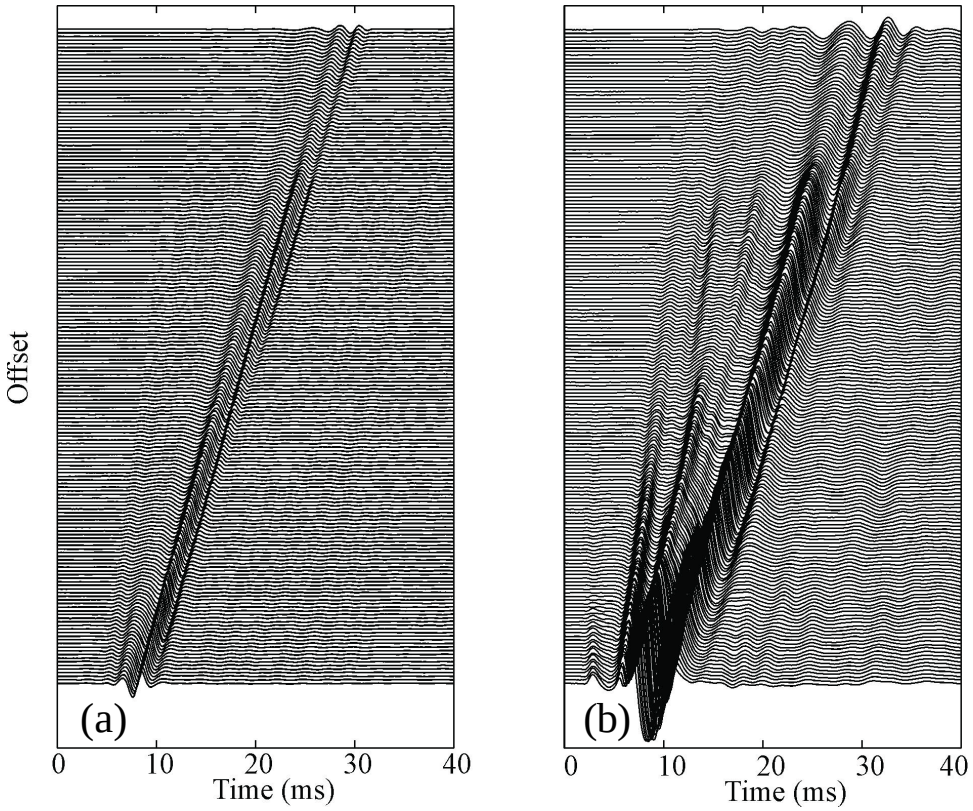

Figure 3: Waterfalls Measured at (a) Low and (b) High Drive Amplitudes.

To study the effects that drive amplitude changes have upon the propagating elastic waves in the experimental model, a second set of measurements was conducted where the surface displacements were measured using nineteen different drive amplitudes over a 54 dB range that extended from the noise floor through the linear regime into the nonlinear regime. Measurements were made at four distances from the elastic wave source (44, 104, 164, and 224 cm) by averaging 1000 differentiated Gaussian pulses with a center frequency of 450 Hz; the data are presented in Figure 4a for measurements without buried objects in the scan region and in Figure 4b for measurements with an anti-personnel landmine buried 0.75 cm deep and 104 cm from the elastic wave source. Each column shows the Rayleigh surface wave measured at a given location as noted above the column. Each trace contains 15 ms of data (time offset as indicated below each column) and was normalized by its drive amplitude to facilitate the comparison of pulse shapes. The vertical separation between traces indicates a 3 dB increase in drive amplitude where the bottom trace was measured at the lowest drive amplitude and the top trace was measured at the highest drive amplitude.

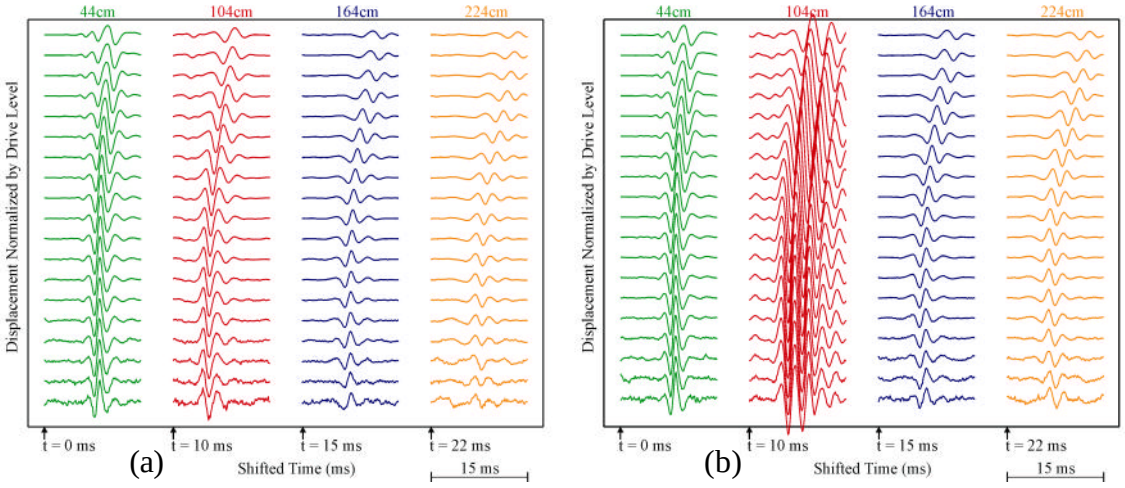

Figure 4: Surface Displacements Measured as a Function of Drive Amplitude and Propagation Distance in the Experimental Model (a) Without Buried Objects and (b) With an Anti-Personnel Landmine Buried 0.75 cm Deep, 104 cm from the Elastic Wave Source.

In Figure 4a, linear dispersion is apparent in the change of the pulse shapes as a function of measurement distance at the lower drive amplitudes. This is most likely due to the depth-dependent material properties of the experimental model. Pulse shape changes as a function of drive amplitude at each measurement location are evidence of nonlinear dispersion. Losses increase with the drive amplitude due to the hysteresis of the stress-strain relationship of the medium in the nonlinear regime. Additionally, wave speed slowing as a function of drive amplitude is observed at each measurement location. This slowing effect in soils has been attributed to the changes in the soil properties due to high amplitude waves[9]. In Figure 4b, the resonance of the landmine and surface layer of soil increased the measured surface displacements at the second measurement location; similar trends of linear dispersion, nonlinear dispersion, and wave speed slowing are apparent in the data. To determine the transition point from the linear to nonlinear regime, the root-mean-squared displacement of a time window containing the dominant surface waves was plotted as a function of drive signal amplitude in Figure 5. The noise floor apparent in the time domain traces at the lowest drive amplitudes in Figure 4 occurs at 20 to 25 dB in Figure 5. When the system enters the nonlinear regime at the higher drive amplitudes, nonlinear saturation occurs as additional energy cannot be imparted to the elastic waves. In the linear regime, each increase in drive signal amplitude incurs a proportional increase in the measured surface displacements; this is not the case in the nonlinear regime as the soil cannot support the higher amplitude waves.

While the radar sensor provides a non-invasive measurement of the normal surface displacements of the propagating waves in the scan region, no information can be obtained regarding the in-plane particle motion. Buried accelerometers and surface-coupled geophones have been used in the experimental model and at the field test site to measure the particle motion on three orthogonal axes. In the first measurements conducted in the laboratory experimental model using the triaxial accelerometers, the

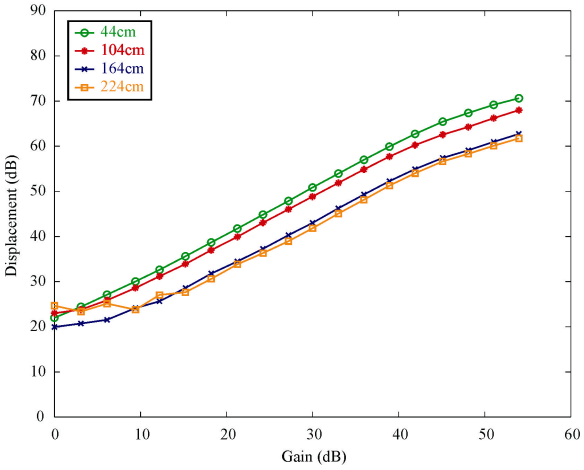

Figure 5: Root-Mean-Squared Displacements as a Function of Drive Amplitude for Averaged Pulses Measured at Four Distances from the Elastic Wave Source in the Experimental Model Without Buried Objects.

depth-dependence of the Rayleigh wave[9] has been observed. Two linear arrays were buried in the experimental model; the first used seven accelerometers and was 0.5 cm below the surface while the second used eight accelerometers and was 21.5 cm below the surface. The first accelerometer in the surface array was located 30 cm from the elastic wave source while the first accelerometer in the deep array was directly below the elastic wave source. Both arrays were configured with 30 cm between adjacent accelerometers for a total range of 2.1 m. In Figure 6, the depth-dependence of the Rayleigh wave is shown in the hodograms plotted for the last accelerometer in the surface array (Figure 6a) and in the deep array (Figure 6b). In the top plots in Figure 6, the vertical and horizontal particle motion has been plotted as a function of time. The four hodograms shown in Figures 6a and 6b plot the vertical displacement versus the horizontal displacement to show the direction of motion, which is indicated by the arrows. The surface accelerometer measured counter-clockwise (retrograde) particle motion when the Rayleigh wave passed the measurement location whereas the deeper accelerometer measured clockwise (prograde) particle motion at the same time. This change from retrograde to prograde motion is indicative of the Rayleigh wave's depth-dependence. The deeper accelerometer also measured a compressional wave propagating at approximately 200 m/s, which is in agreement with published measurements of P-wave speeds in sand[10, 11]; the first hodogram of this arrival shows predominantly horizontal particle motion in Figure 6b.

Field measurements were conducted using a surface array of sixteen accelerometers that ranged from 45 cm to 2.75 m from the elastic wave source. The accelerometers were buried approximately 0.5 cm deep; installation of a deeper array similar to the one used in the experimental model was not possible at the field site due to the existing soil conditions. The hodogram of the measured particle motion using the surface array at the field test site shown in Figure 7 indicates similar motion to that

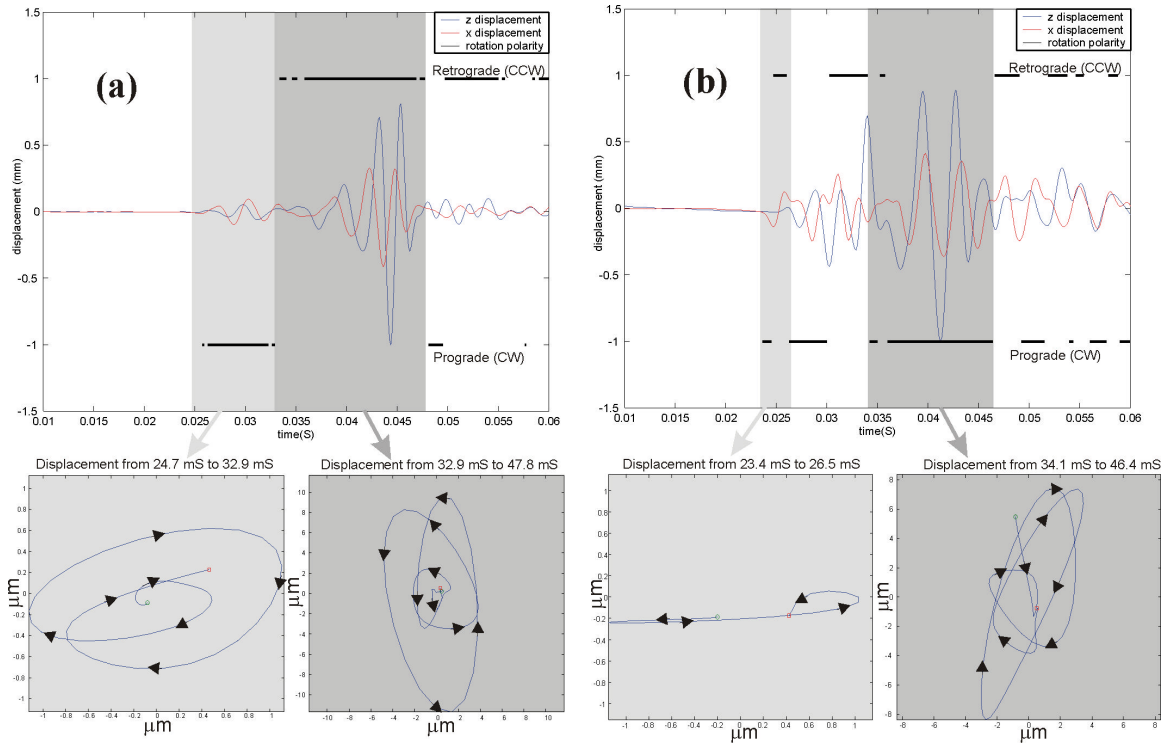

Figure 6: Depth-dependence of Rayleigh Wave as Observed in Differences in Particle Motion (a) 0.5 cm and (b) 21.5 cm Below the Surface in the Experimental Model.

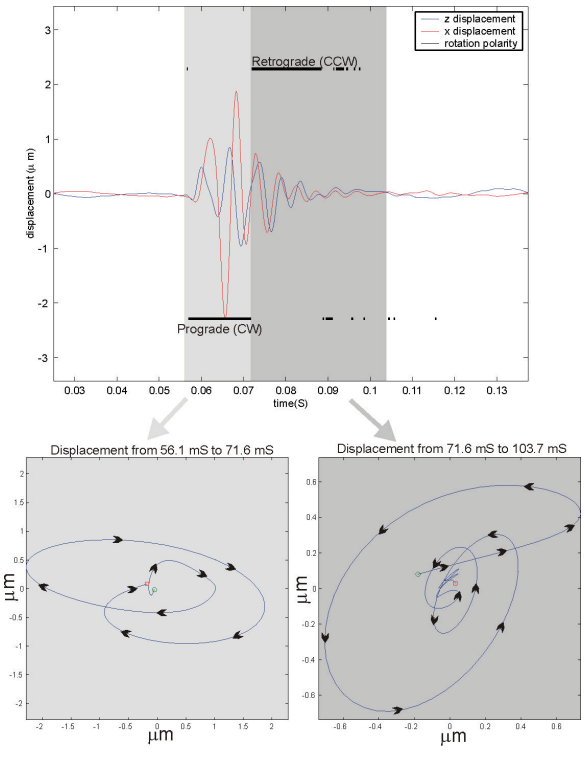

Figure 7: Particle Motion Measured at the Field Test Site (x = 2.75 m, z = 0.5 cm).

measured by the surface accelerometers in the laboratory experimental model in Figure 6a.

The Rayleigh wave can be seen to propagate along the soil surface in the waterfalls of the vertical and horizontal accelerations measured with the surface array in Figure 8. For these measurements, a differentiated Gaussian pulse with a center frequency of 400 Hz was averaged 1000 times to increase the signal-to-noise ratio (SNR). Each trace in Figure 8 was measured by an individual channel of a triaxial accelerometer and was normalized by its own peak amplitude for examination of pulse shape changes as a function of propagation distance. The vertical spacing between traces in Figure 8 indicates the separation distance between the accelerometers in the array as configured at the field test site. Figure 8a shows the acceleration normal to the soil surface while Figure 8b shows the acceleration in the horizontal direction away from the elastic wave source (orthogonal to the surface normal). By tracking the peaks and troughs in waterfall plots similar to those shown in Figure 8, wave propagation speeds were calculated that ranged from 384 m/s on the leading edge to 129 m/s on the trailing edge of the pulse. However, identification of individual wave types is difficult due to the complicated interactions of multiple wave types in a medium containing layering and inhomogeneities. By plotting the retrograde and prograde nature of the pulses in waterfall fashion in Figure 9, a fast wave propagating at approximately 270 m/s and the Rayleigh wave propagating at approximately 135 m/s can be identified. The faster wave speed of 270 m/s is inherently low due to geometrical spreading and absorption; the SNR of the measurements of the arrival of the fast wave were not sufficient to accurately determine the wave speed. However, the SNR was higher for the arrival of the Rayleigh wave, which made it possible to accurately determine the propagation speed as 135 m/s. Radar measurements at the same field site[4] also found that the Rayleigh wave propagates at 135 m/s.

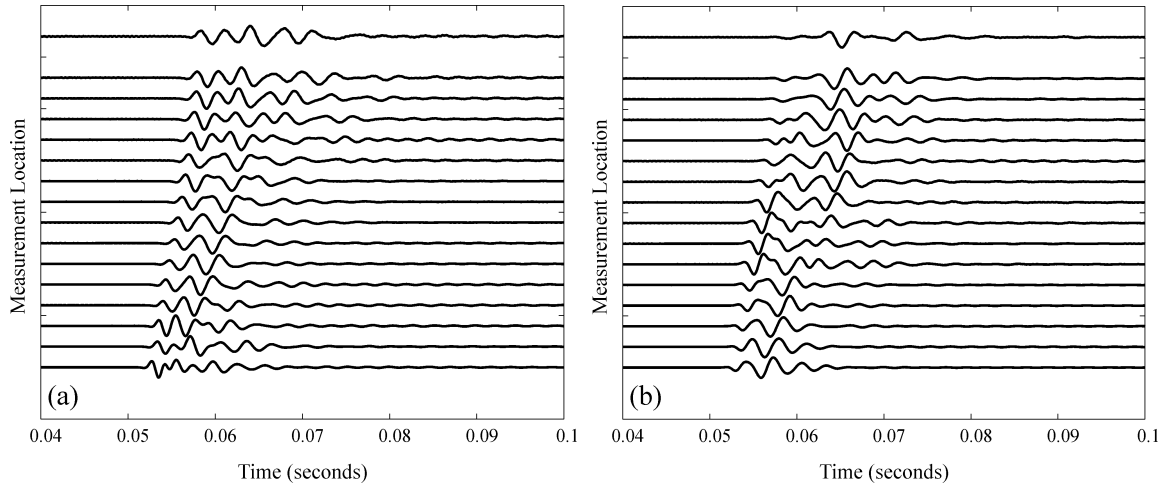

Figure 8: Propagation of Differentiated Gaussian Pulses at the Field Test Site in the (a) Vertical and (b) Horizontal Directions.

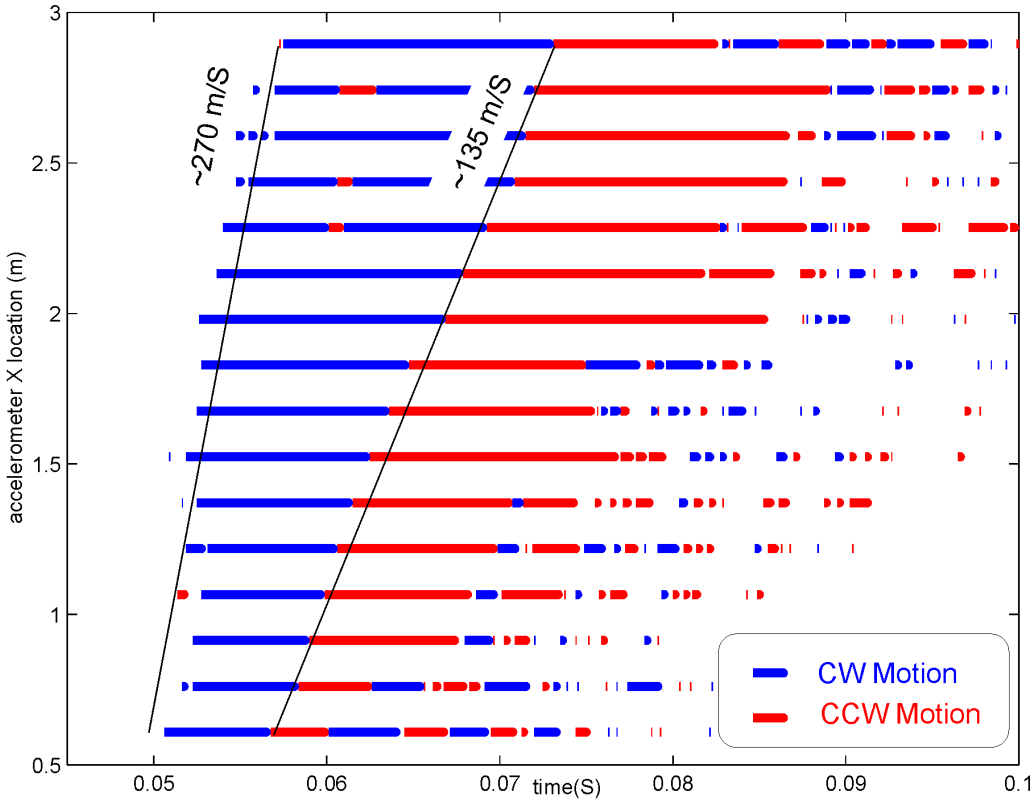

Figure 9: Polarity Changes Measured by Surface Accelerometer Array at Field Test Site.

CONCLUSIONS

Elastic wave propagation measurements in a laboratory experimental model and a field test site have shown similar propagation characteristics despite widely different soil compositions and environmental conditions. The well-weathered mixture of sand, silt, and clay at the field test site was a much stiffer medium than the damp, compacted sand of the experimental model. As such, the wave propagation speeds measured at the field test site were higher than the corresponding speeds measured in the experimental model. The presence of multiple soil materials, layering, and inhomogeneities complicated the propagating wave field at the field test site in comparison to the soil in the experimental model. While the experimental model represents a more homogeneous medium, there are still variations in the material properties as a function of depth and a water table, both of which affect the propagation of elastic waves.

ACKNOWLEDGEMENTS

This work was supported by the Office of Naval Research under Contract Numbers N00014-01-1-0743 and N00014-99-1-0995.

REFERENCES

1. Scott, W. R., Jr., J. Martin, and G. Larson, "Experimental Model for a Seismic Landmine Detection System," IEEE Transactions on Geoscience and Remote Sensing, vol. 39, no. 6, June 2001, pp. 1155-1164.
2. Scott, W.R., Jr., Schröder, C., and Martin, J.S., "An Acousto-Electromagnetic Sensor for Locating Land Mines," Proceedings of the SPIE, vol. 3392, *Detection and Remediation Technologies for Mines and Minelike Targets III*, Orlando, FL, pp. 176-186, April 1998.
3. Scott, W. R., Jr., S. Lee, G. D. Larson, J. S. Martin, and G. S. McCall II, "Use of High-Frequency Seismic Waves for the Detection of Buried Land Mines," Proceedings of the SPIE, vol. 4394, April 2001.
4. Scott, W. R., Jr., S. H. Lee, P. H. Rogers, J. S. Martin, G. D. Larson, and G. S. McCall, II, "Technical Issues Associated with the Detection of Buried Landmines with High-frequency Seismic Waves," Proceedings of SPIE, vol. 4372, April 2002.
5. Larson, G. D., J. S. Martin, W. R. Scott, Jr., and G. S. McCall II, "Environmental Factors that Impact the Performance of a Seismic Land Mine Detection System," Proceedings of SPIE, vol. 4394, April 2001.
6. Schröder, C. T., "On the Interaction of Elastic Waves with Buried Land Mines: an Investigation Using the Finite-Difference Time-Domain Method," Ph.D. Dissertation, School of Electrical and Computer Engineering, Georgia Institute of Technology, Atlanta, GA, July 2001.
7. Jordan, T., and Thomson, S. D., S&ME Project Report No. 1651-01-248, January 3, 2002.
8. Schröder, C. T., and W. R. Scott, Jr., "On the Complex Conjugate Roots of the Rayleigh Equation: the Leaky Surface Wave," J. Acoust. Soc. Amer. **110** (6), December 2001, pp. 2867-2877.
9. Santamarina, J. C., K. A. Klein, and M. A. Fam, Soils and Waves: Particulate Materials Behavior, Characterization, and Process Monitoring, John Wiley & Sons, Ltd., Chichester, England, 2001.
10. Bachrach, R., and A. Nur, "High-Resolution Shallow-Seismic Experiments in Sand, Part I: Water Table, Fluid Flow, and Saturation," Geophysics, vol. 63, no. 4, July-August 1998, pp. 1225-1233.
11. Bachrach, R., J. Dvorkin, and A. Nur, "High-Resolution Shallow-Seismic Experiments in Sand, Part II: Velocities in Shallow Unconsolidated Sand," Geophysics, vol. 63, no. 4, July-August 1998, pp. 1234-1240.